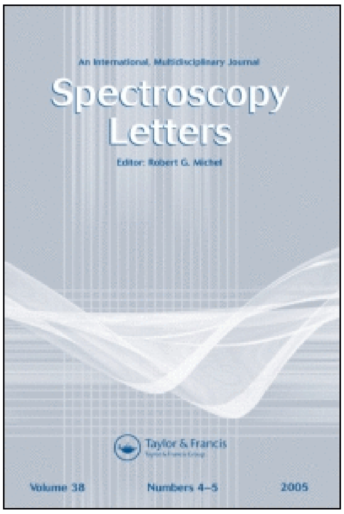

Spectroscopy Letters
Publication details, including instructions for authors and subscription information:
http://www.informaworld.com/smpp/title~content=t713597299

Light Emission and Scanning Electron Microscopic Characterization of Porous Silicon

K. Berrada[a]; H. Targaoui[a]; A. Kaddouri[a]; G. Louarn[b]; G. Froyer[b]; A. Outzourhit[c]
[a] Département de Physique, Faculté des Sciences Semlalia, SIAM, Marrakech, Morocco [b] LPMN, Institut des Matériaux Jean Rouxel, Nantes Cedex, France [c] Département de Physique, Faculté des Sciences Semlalia, LPSCM, Marrakech, Morocco

To cite this Article Berrada, K. , Targaoui, H. , Kaddouri, A. , Louarn, G. , Froyer, G. and Outzourhit, A.(2007) 'Light Emission and Scanning Electron Microscopic Characterization of Porous Silicon', Spectroscopy Letters, 40: 5, 753 — 762
To link to this Article: DOI: 10.1080/00387010701429351
URL: http://dx.doi.org/10.1080/00387010701429351

Spectroscopy Letters, 40: 753–762, 2007

ISSN 0038-7010 print/1532-2289 online
DOI: 10.1080/00387010701429351

Light Emission and Scanning Electron Microscopic Characterization of Porous Silicon

K. Berrada, H. Targaoui, and A. Kaddouri
SIAM, Département de Physique, Faculté des Sciences Semlalia, Marrakech, Morocco

G. Louarn and G. Froyer
LPMN, Institut des Matériaux Jean Rouxel, Nantes Cedex, France

A. Outzourhit
LPSCM, Département de Physique, Faculté des Sciences Semlalia, Marrakech, Morocco

Abstract: Optical emission resulting from sputtered species during ion bombardment of porous and oxidized porous silicon targets has been studied. Samples were bombarded with 5-keV Kr^{+} ions at an incidence angle of 70 degrees, and the light emitted was analyzed over the wavelength range 200–300 nm. The surface morphology was investigated, and the micrographs revealed grooves parallel to the plane of incidence when the porosity was surprisingly observed in the grooves under each pore. The results are discussed as a function of the incidence angle and the porosity of the silicon targets.

Keywords: Light emission, oxidized silicon, porosity, porous silicon, SEM, sputtering

Received 27 September 2006, Accepted 5 March 2007

The authors were invited to contribute this paper to a special issue of the journal entitled "Research on Spectroscopy in Morocco." This special issue was organized by Miguel de la Guardia, Professor of Analytical Chemistry at Valencia University, Spain.

Address correspondence to K. Berrada, SIAM, Département de Physique, Faculté des Sciences Semlalia, BP 2390, Marrakech, Morocco. E-mail: berrada@ucam.ac.ma

INTRODUCTION

In recent years, porous silicon (PS) has received considerable attention due to its interesting properties.[1–7] Some studies focused on the emission of light from sputtered and scattered excited particles as well as from the solid under energetic ion bombardment.[8,9] However, to our knowledge, no studies on PS layers morphology were performed after ion bombardment.

In this work, we present some light emission results from PS and oxidized PS surfaces during 5-keV Kr^+ ion bombardment at room temperature. The experiment was performed with an optical emission spectrometer installed at the Cadi Ayyad University in Marrakech. The light emission caused by the ion–surface interaction is technically referred to as the beam-induced light emission (BLE) or sputtered ions photons spectroscopy (SIPS).[10,11] In our team, this optical emission method is developed under the acronym ASSO (Analyse de Surfaces par Spectroscopie Optique).

After ion bombardment, scanning electron microscopy (SEM) was used to study the surface morphology of ion-irradiated PS at oblique incidence. An attempt was made to understand the observed morphology in terms of various processes that occur during ion bombardment.

MATERIALS AND METHODS

Porous silicon was obtained by an electrochemical anodization of (100)-oriented single crystalline silicon in 20% hydrofluoric acid solution in ethanol. The anodization was carried out at room temperature on highly doped p-type silicon wafers ($\rho = 3$ to $7\ m\Omega cm$). The imposed anodic current density was $100\ mAcm^{-2}$, and under these conditions the porous layer is 10 μm thick after 240 s with 80% porosity.[12] The samples were rinsed with distilled water several times, then with ethanol before drying and subsequently treated for few seconds in NaOH or in SF_6 plasma. Oxidized silicon was obtained by double oxidation at very high temperatures following the receipt reported by Guendouz et al.[13]

The targets were mounted inside a high vacuum chamber on a sample holder that can rotate to change the angle of incidence and also permit a translation of samples. The ion beam was incident at 70 degrees with respect to the sample surface normal. The target chamber was pumped separately by a 500 L/s turbomolecular pump backed by a diaphragm pump. The gas pressure was measured by a Penning gauge (Balzers TPG 300)and the residual pressure was about 10^{-7} mbar. The emitted light was analyzed through a R320 Jobin-Yvon monochromator equipped with an 1800 grooves holographic grating. The analyzed light was transmitted to a Hammatsu R4220P photomultiplier, and the experiment was controlled by a microcomputer. A more detailed experimental setup has been described earlier.[14]

Table 1. Experimental conditions for recording the ASSO luminescence spectra

Angular position	70 degrees
Pressure	$<10^{-7}$ mbar
Monochromator fonts	400 μm
Spectral range	200–300 nm
Resolution	0.30 nm
Time	1 s
Current sample	0.5–0.6 μA
Ions energy	5-keV

The beam-induced light emission method was recently used in a study of the surface of the binary alloy AlMg.[15] Its particularly adapted to follow the oxide coatings that are formed on the samples after introduction of the O_2 gas under controlled pressure. Ghose et al.[16] studied the effect of the layers of SiO_2 that are formed in the presence of oxygen on silicon substrates. In our experiments, the single-crystalline silicon, PS, and oxidized PS samples are placed in a vacuum enclosure with a pressure better than 10^{-7} mbar. The light signal is studied as a function of the energy of the incident ions and the angular position of the sample-target relatively to the incident beam. The wavelength range explored in this study extends from 200 to 300 nm with spectral resolution of 3 Å.

Samples are initially bombarded to eliminate the surface oxide layers that can be formed after their fabrication. The stabilization of the visible signal is obtained after a few minutes. After this step, the emitted particles reflect the chemical composition of the volume of the sample. The experimental conditions under which we recorded our spectra are summarized in Table 1. The photon yield or intensity was measured in photon counts per second.

The morphology of treated PS and oxidized PS surfaces before and after ion beam bombardment was observed by SEM. In a detailed SEM investigation, we will show that ion beam bombardment at oblique incidence $\theta = +70$ degrees results in significant modifications of the structures of the surfaces. The SEM experiments were performed at the Jean Rouxel Materials Institute (Nantes, France).

RESULTS AND DISCUSSION

Figures 1, 2, and 3 show typical emission spectra obtained from 5-keV Kr^+ ion-beam bombardment of silicon, PS, and oxidized PS, respectively. All the spectra were recorded at a base pressure of $\sim 10^{-7}$ mbar. The light intensity first rises sharply and then declines exponentially. For our samples, it takes a few minutes ($\sim$10 min) to settle down to steady value as shown in Ref. 17. For PS (Fig. 2) and oxidized PS (Fig. 3), 10 atomic lines

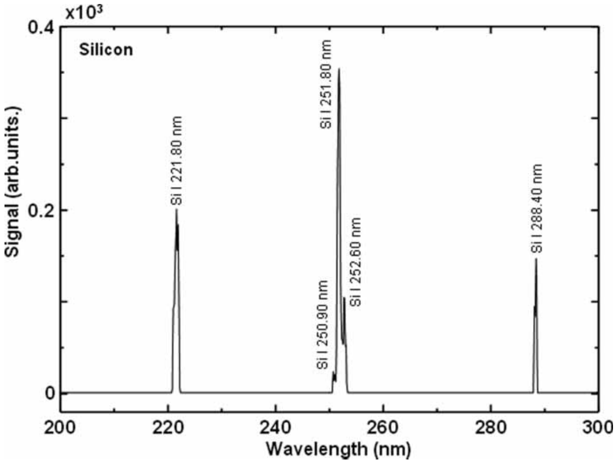

Figure 1. Photon spectrum after 5-keV Kr^+ ion bombardment of Si.

are observed under these experimental conditions and attributed to neutral Si I. Some of these atomic lines are totally absent in the silicon target spectra (Fig. 1). The attribution of wavelengths and intensities of principal atomic lines observed are reported in Table 2. The corresponding atomic transitions are also presented.

The measured wavelength values are in perfect agreement with those found in the literature when a correction of approximately 0.2 nm is taken into account. This systematic shift is due to the calibration of the stepper motor that controls the wavelengths of the monochromator.

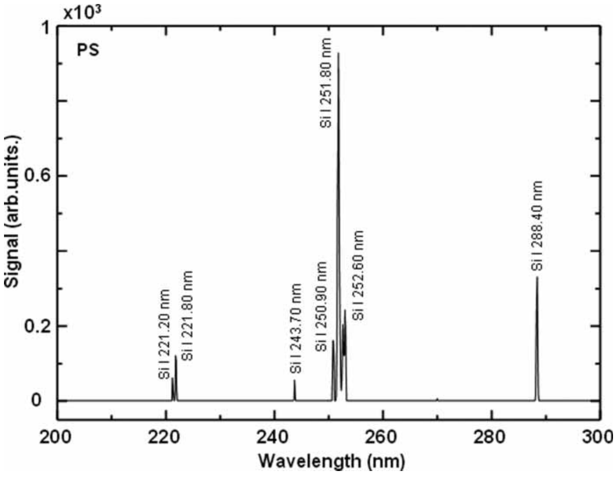

Figure 2. Photon spectrum after 5-keV Kr^+ ion bombardment of PS.

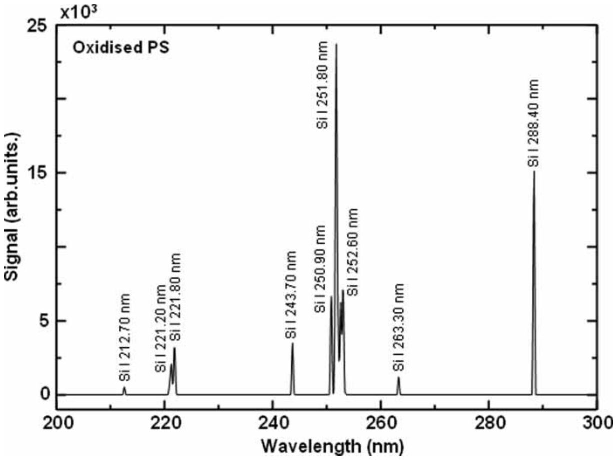

Figure 3. Photon spectrum after 5-keV Kr^+ ion bombardment of oxidized PS.

The absolute intensity (counts per second) of the Si I lines is higher in the case of PS (Fig. 2) and oxidized PS (Fig. 3) samples than in the silicon (Fig. 1) substrates. However, it is more pronounced in the oxidized PS substrates. The results suggest that both porosity and oxidation result in an increase of the signal. Oxidation is responsible for increase in the intensities of the lines when one passes from silicon to oxidized silicon as observed in our previous work.[8] It also seems that the porosity reinforces the fast oxidation of the pores on the surface and increases the intensity of the signal.

The change in the intensities of the spectral lines as a function of the nature of the sputtered surface can be explained by the interaction of this surface with the excited species formed in its vicinity. In the framework of the electron exchange model,[18] this interaction leads to a competition between the radiative and nonradiative transitions of the excited species.

Table 2. The strongest identified lines in PS, under 5-keV Kr^+ impact, in the 200–300 nm range

λ_{mes} (nm)	λ_{lit} (nm)	$\Delta\lambda$ (nm)	Transition
221.2	221.0	0.20	Si I: $3s\ 3p^3\ {}^3D^0_2 - 3s^2\ 3p^2\ {}^3P_1$
221.8	221.66	0.14	Si I: $3s\ 3p^3\ {}^3D^0_3 - 3s^2\ 3p^2\ {}^3P_2$
243.7	243.51	0.19	Si I: $3s^2\ 3p\ 3d\ {}^1D^0_2 - 3s^2\ 3p^2\ {}^1D_2$
250.9	250.69	0.21	Si I: $3s^2\ 3p\ 4s\ {}^3P^0_2 - 3s^2\ 3p^2\ {}^3P_1$
251.8	251.61	0.19	Si I: $3s^2\ 3p\ 4s\ {}^3P^0_2 - 3s^2\ 3p^2\ {}^3P_2$
252.6	252.41	0.19	Si I: $3s^2\ 3p\ 4s\ {}^3P^0_0 - 3s^2\ 3p^2\ {}^3P_1$
288.4	288.16	0.24	Si I: $3s^2\ 3p\ 4s\ {}^1P^0_1 - 3s^2\ 3p^2\ {}^1D_2$

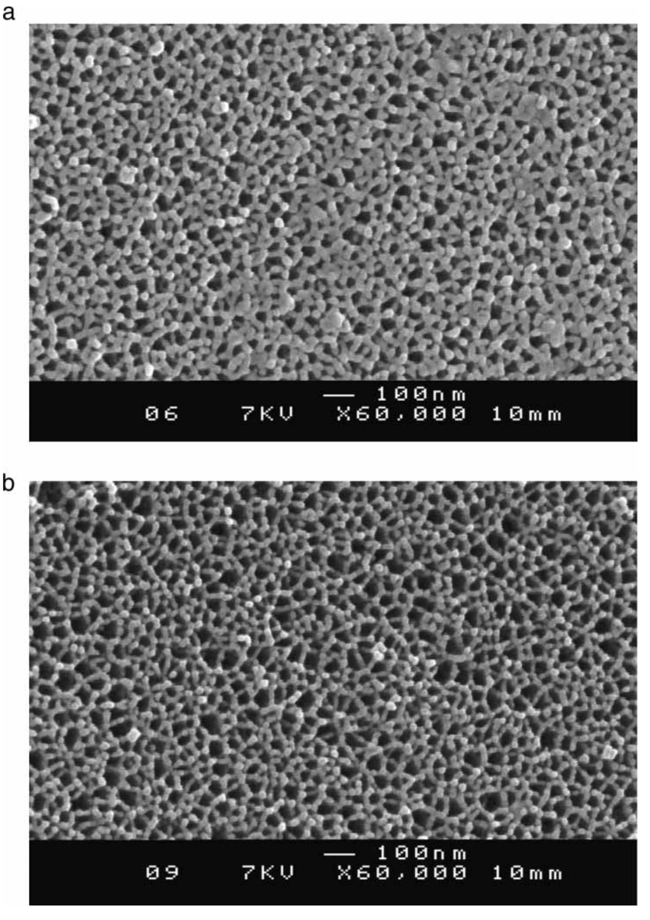

Figure 4. (a) Morphology after anodization of p-type substrate as reported for the experimental conditions of PS. (b) Morphology after anodization of p-type substrate as reported for the experimental conditions of oxidized PS.

Clearly, the porosity and the oxidation of silicon targets lead to significantly higher line intensities, suggesting an increased number of radiative transitions in this case. The role of the oxidized surface in PS is not completely understood. There have been some attempts made to explain this effect in terms of an inhibition of possible radiation-less de-excitation, due to the band gap in the SiO_2 porous oxide.[16]

The microstructure of PS was investigated using SEM. Figure 4 shows micrographs of PS (a) and oxidized PS (b). The anisotropic structure of the porous layers can be clearly seen. The porosity is presented in the form of a network of pores separated by single-crystalline silicon. Particularly oxidized PS shows well-defined pore structure and pore distribution. In our

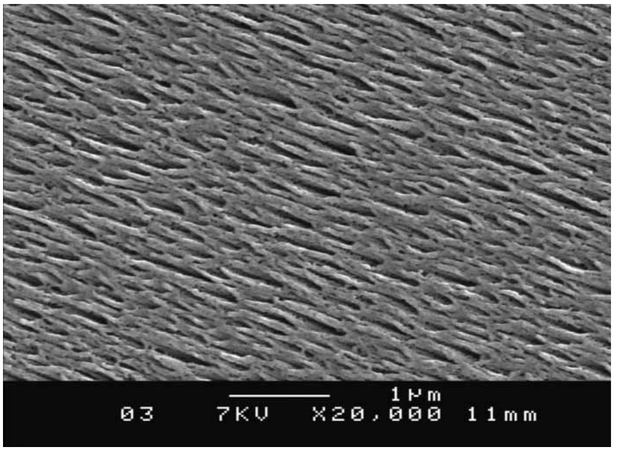

Figure 5. A typical micrograph of the PS surface after 30-min ion bombardment (×20,000).

conditions, the pore diameter ranges from 20 to 50 nm and the porous layer is 10 μm thick after 240 s.[19] On the other hand, electron diffraction showed that the walls of the pores keep the orientation of single-crystalline silicon.[2]

The pore structure on the surfaces after ion beam bombardment is shown on the SEM micrographs of Fig. 5 (for PS with a magnification ×20,000) and Fig. 6 (for oxidized PS with a magnification ×60,000). Experiments were realized at an incidence angle $\theta = +70$ degrees with respect to the sample surface normal. For the SEM image shown in Fig. 5, it can be clearly seen that the new orientation of

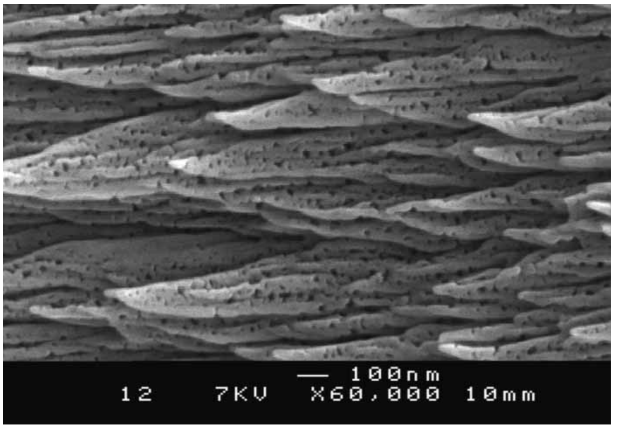

Figure 6. A typical micrograph of oxidized PS surface after 30-min ion bombardment (×60,000).

the pores on the surfaces of the porous layers is in the direction of the incidence angle of the ion beam. Particularly, it appears that the pore structure is oriented in the plane of incidence of the ion beam. Needle-like features oriented in the direction of the incidence was observed by Fournier et al.[20] on smooth surfaces of beryllium targets under 5-keV krypton beam. In our case, it seems that the ion beam reoriented the columns structures of the PS surface in the direction of incidence of the ion beam. To our knowledge, such an effect has never been observed or reported on PS layers before.

The ion-beam sputtering has also revealed the internal structure of the PS pores. What has surprised us in these observations is the presence of pores on the internal surface of the long porous columns that form on the surface of the substrates. To our knowledge, no published works have observed such features on PS using ion-beam sputtering. This result, which is obtained using oblique incidence ion-beam abrasion of porous surfaces, could have a repercussion on the preceding studies carried out on porous silicon substrates such as the estimation of the specific surface areas from the pore diameter and pore depth only. The origin of the observed pores within the columns is not yet understood. It may be due to the initial attack by HF or induced by ion-beam sputtering.

Further analysis by SEM of cross sections of the sputtered areas of PS substrates could be used to determine the penetration depth of the ion beam in the surfaces of porous layers. The study by SEM of PS and oxidized PS silicon surfaces after attack by ion beam will allow one to follow the internal morphology of the pores.

CONCLUSIONS

Light emission under 5-keV Kr^+ ion bombardment of PS and oxidized PS layers was analyzed in the 200–300 nm wavelength range. The results suggest that the enhancement of intensity of the spectral lines is caused by the oxidation of the pores. For PS, the photon yield increases instantaneously to a high value as in the case of the sputtering of oxygen-rich surfaces.

The structure and morphology of the pores were followed by SEM. We have shown that after ion bombardment at oblique incidence, the PS layers take an orientation following the plane incidence of the ion beam.

Thanks to ion bombardment, we also observed porous structure inside the column pores. This result makes it possible to increase specific surface at the time of the filling of the pores by active materials necessary to the fabrication of composites.

ACKNOWLEDGMENTS

The authors express their gratitude to CNRST-Morocco and CNRS-France for their financial support in the project (Ref. 17702 and Chimie 10/05). We are also very grateful to Prof. Serge Lefrant from Institut des Matériaux Jean Rouxel de Nantes and to Prof. Paul Guy Fournier and Prof. Janine Fournier from Université Paris Sud d'Orsay for their precious collaboration.

REFERENCES

1. Ünal, B.; Parbukov, A. N.; Bayliss, S. C. Photovoltaic proprieties of a novel stain etched porous silicon and its application in photosensitive devices. *Opt. Mater.* **2001**, *17*, 79–82.
2. Errien, N.; Joubert, P.; Chaillou, A.; Mahric, C.; Godon, C.; Louarn, G.; Froyer, G. Electrochemical growth of poly(3-dodecylthiophene) into porous silicon: a nanocomposite with tubes or wires? *Mater. Sci. Eng. B* **2003**, *100*, 259–262.
3. Rivolo, P.; Pirasteh, P.; Chaillou, A.; Joubert, P.; Kloul, M.; Bardeau, J.-F; Geobaldo, F. Oxidised porous silicon impregnate with Congo Red for chemical sensoring applications. *Sensors Actuators B* **2004**, *100*, 99–102.
4. Iraji zad, A.; Rahimi, F.; Chavoshi, M.; Ahadian, M. M. Characterisation of porous poly-silicon as a gas sensor. *Sensors Actuators B* **2004**, *100*, 341–346.
5. Lysenko, V.; Vitiello, J.; Remaki, B.; Barbier, D.; Skryshevsky, V. Nanoscale morphology dependent hydrogen coverage of meso-porous silicon. *Appl. Surf. Sci.* **2004**, *230*, 425–430.
6. Solanki, C. S.; Bilyalov, R. R.; Poortmans, J.; Nijs, J.; Mertens, R. Porous silicon layer transfer processes for solar cells. *Solar Energy Materials and Solar Cells* **2004**, *83*, 101–113.
7. Zhao, Y.; Yang, D.; Li, D.; Jiang, M. Photoluminescence of oxidised porous silicon under UV-light illumination. *Materi. Sci. Eng. B* **2005**, *116*, 95–98.
8. Louarn, G.; Berrada, K.; Errien, N.; Ait El Fqih, M.; Froyer, G.; Kaddouri, A. Vibrational and optical emission spectroscopies of porous and oxidised porous silicon. *Physical and Chemical News* **2005**, *21*, 5–11.
9. Suchanska, M. Ion-induced photon emission of metals. *Prog. Surf. Sci.* **1997**, *54*, 165–209.
10. Thomas, G. E. Bombardment-induced light emission. *Surf. Sci.* **1979**, *90*, 381–416.
11. Fournier, P. G.; Fournier, J.; Bellaoui, B. Optical emissions from sputtering species formed by the fast ion bombardment of clean and oxygenated Mg surfaces. *Nucl. Instrum. Methods Phys. Res. B* **1992**, *67*, 604–609.
12. Charrier, J.; Lupi, C.; Haji, L.; Boisrobert, C. Optical study of porous silicon buried waveguides fabricated from p-type silicon. *Materials Science in Semiconductor Processing* **2000**, *3* (5–1), 357–361.
13. Guendouz, M.; Pédrono, N.; Etesse, R.; Joubert, P.; Bardeau, J.-F.; Bulou, A.; Kloul, M. Oxidised and non oxidised porous silicon/disperse red 1 composite: physical and optical properties. *Phys. Status Solidi (a)* **2003**, *197*, 414–418.
14. Fournier, J.; Fournier, P. G.; Kaddouri, A.; Dunet, H. Optical spectroscopy analysis of $YBa_2Cu_3O_7$ at room temperature and at 10. *K. J. Appl. Phys.* **1991**, *69*, 2382–2387.
15. Berrada, K.; Fournier, J.; Fournier, P. G.; Kaddouri, A. Optical emissions of Al-Mg alloys under krypton ions bombardment. *Physical and Chemical News* **2004**, *17*, 49–53.
16. Ghose, D.; Brinkmann, U.; Hippler, R. Light emission from a Si target during ion beam sputtering. *Surf. Sci.* **1995**, *327*, 53–58.

17. Bhattacharyya, S. R.; Brinkmann, U.; Hippler, R. Investigation of relative sputtering yields during ionoluminescence of Si. *Appl. Surf. Sci.* **1999**, *150*, 107–114.
18. Vege, E. Study of atomic excitations in sputtering with the use of Mg, Al, Ca and Cd targets. *Phys. Rev. B* **1983**, *28*, 5029–5036.
19. Errien, N. *Réalisation et étude de composite à base de silicium poreux ou de silice porouse-polymère conjugué pour l'obtention de matériaux pour le traitement tout optique du signal*; Thèse de Doctorat de l'Université de Nantes: France, 2004, 240 pp.
20. Fournier, P.-G.; Nourtier, A.; Shulga, V. I.; Ait El Fqih, M. Angular distribution of sputtered particles and surface morphology: The case of beryllium under krypton beam at various incidences. *Nucl. Instrum. Methods Phys. Res. B* **2005**, *230* (1–4), 577–582.